Exploring the impact of the dissipation coefficient in warm Higgs inflation

Wei Cheng,[1,*] Xue-Wen Chen,[2,†] Ruiyu Zhou,[1,‡] Jiu-Jiang Jiang,[1] Xin-Rui Dai,[1] Zi-Han Zhang,[1] and Tong Qin[1]
[1]*School of Science, Chongqing University of Posts and Telecommunications, Chongqing 400065, China*
[2]*Chongqing University of Science and Technology, Chongqing 401331, China*

(Received 23 January 2024; accepted 21 March 2024; published 9 April 2024)

In this study, we conduct a detailed analysis of the dissipation coefficient (Q) of warm Higgs inflation (WHI), which exerts important influences on the entire warm inflation process. By deriving the relationships between various quantities and Q, one can avoid *a priori* assumptions, i.e., strong dissipation ($Q \gg 1$) or weak dissipation ($Q \ll 1$). Taking into account the constraints imposed by the cosmic microwave background, the dissipation the coefficient Q remains at extremely low levels throughout the entire warm inflation process, i.e., $Q \ll 1$. This observation indicates that WHI falls under the category of weak dissipation warm inflation. Despite being weak dissipation, Q still plays a non-negligible role in the evolution of temperature, energy, and other quantities. We delve into the impact of the primordial power spectrum on the dissipation coefficient Q during the warm inflation process, discovering that the dependency is not significant. Consequently, this results in a weak sensitivity of the gravitational wave spectrum ($\Omega_{\mathrm{GW},0}h^2$) to changes in Q. In addition, the variation of tensor-to-scalar ratio r has a significant effect on the $\Omega_{\mathrm{GW},0}h^2$ of cold inflation and a small effect on WHI. Finally, gravitational waves generated by WHI hold the potential for verification in future observational experiments, especially through the SKA100 experiment.

DOI: 10.1103/PhysRevD.109.083509

I. INTRODUCTION

Inflationary cosmology has emerged as the pivotal framework for understanding the dynamics of the early Universe, addressing fundamental issues such as the flatness, and the horizon problems [1–3], while providing a mechanism to explain the inhomogeneities observed by Planck and WMAP in the cosmic microwave background radiation (CMB) [4]. Within this cosmological paradigm, two principal models of inflation have been distinguished: cold inflation [5–17] and warm inflation [18–26].

Although the cold inflation model (CI) has achieved significant success in depicting the exponential expansion of the Universe and the generation of density perturbations due to quantum fluctuations of the inflation field [27–34], it falls short in explaining the transition from inflationary to radiation dominated era [35–40]. In contrast, the warm inflation model introduces a new mechanism that maintains thermal equilibrium and continuous production of relativistic particles [21,22,24,41–52], offering a more seamless transition from the inflationary phase to a radiation-dominated stage [53–57]. A recent review of warm inflation has been discussed in Refs. [58,59].

Among the plethora of models for warm inflation, the warm Higgs inflation (WHI) has garnered extensive attention in the scientific community [60–62]. First, Higgs Inflation (HI) garners attention for its integration of the Higgs field, within the Standard Model, with the early Universe's rapid expansion, offering a succinct and economical solution to explain the Universe's flatness, and horizon. This approach circumvents the need for introducing new particles or fields, while providing specific predictions that can be validated through cosmological observations. It not only enhances our understanding of the early Universe but also opens avenues for exploring physics beyond the Standard Model, closely linking particle physics with cosmological studies. Then, WHI not only incorporates the unique properties of the Higgs field but also explores its complex interactions with the inflationary process and dissipative phenomena. Given the pivotal role of the Higgs field in the Standard Model, especially in imparting mass to fundamental particles, its involvement in the warm inflation framework adds complexity and depth to our understanding of the early Universe's dynamics.

This study focuses on a detailed analysis of the dissipation coefficient denoted as Q—within the framework of the WHI. We do not assume *a priori* assumptions in our calculations, whether it be strong dissipation ($Q \gg 1$) or weak dissipation ($Q \ll 1$) [60–62]. Instead, the influence of Q is fully considered and retained throughout the entire

*Corresponding author: chengwei@cqupt.edu.cn
†Corresponding author: chenxuewen@cqust.edu.cn
‡Corresponding author: zhoury@cqupt.edu.cn

computation process. Subsequently, the results of theoretical calculations decide which mechanism is more suitable for describing WI. Specifically, this study explore the dynamical characteristics of Q and its impact on the early Universe's temperature, energy, and other physical quantities, as well as its intricate relationship with the primordial power spectrum. Moreover, this research will investigate the dependency of the gravitational wave power spectrum on Q during WHI, particularly considering the verification prospects in future observational experiments, such as the SKA100 project [63]. The goal of this study is to provide a understanding the physical processes of the early Universe's evolution under the WHI framework.

The rest parts are arranged as follows: In Sec. II, a overview of the background evolution of WHI is presented. Subsequently, the Q-dependent WHI and the Q-dependent relic gravitational waves are investigated. Section III conducts a numerical discussion, encompassing the dynamic evolution of various quantities throughout the WHI process. We also investigate the relationship between the spectral index and tensor-to-scalar ratio, along with the Q-dependent relic gravitational waves. Finally, Sec. IV provides a succinct summary.

II. DISSIPATION COEFFICIENT Q

A. Background evolution of warm Higgs inflation

This section provides a detailed exposition of the background evolution of WHI, aiming to understand the dynamics of the Universe during this period and laying the foundation for the subsequent examination of the dissipation coefficient's influence. The evolution of various energy components in the Universe is governed by the Friedmann equation. Considering the Einstein frame action with the flat FLRW line element, the Friedmann equation for WHI can be formulated as

$$H^2 = \frac{1}{3M_p^2}(\rho_h + \rho_r), \tag{2.1}$$

where the evolution equations for the homogeneous Higgs inflaton field energy (ρ_h) and the radiation energy (ρ_r) can be derived by separately, analyzing the corresponding field motion equations. Specifically, in the context of WHI, their explicit forms are given by

$$\dot{\rho}_h + 3H(\rho_h + p_h) = -\Gamma(\rho_h + p_h), \tag{2.2}$$

$$\dot{\rho}_r + 4H\rho_r = \Gamma\dot{h}^2, \tag{2.3}$$

where the pressure p_h is defined as $p_h = \dot{h}^2/2 - U(h)$, and $\rho_h + p_h = \dot{h}^2$. The general form of the Γ is given by [44,64–66]

$$\Gamma = C_m \frac{T^m}{h^{m-1}}, \tag{2.4}$$

where C_m is associated to the dissipative microscopic dynamics, which is a measure of inflaton dissipation into radiation. Different choices of integer m yield different physical descriptions, e.g., Refs. [64–66]. Within the high temperatures regime, the thermal corrections of the catalyst field mass become significant, leading to a direct proportionality between Γ and temperature T, which implies that $m = 1$ [47,65]. As the dissipative coefficient $Q = \Gamma/(3H)$, the dissipation coefficient Q is directly affected, which ultimately affects whether the model is a strong or weak dissipative model.

In slow-roll scenario, Eqs. (2.2) and (2.3) can be further reduced to

$$3H(1+Q)\dot{h} \simeq -U_h, \tag{2.5}$$

$$4\rho_r \simeq 3Q\dot{h}^2. \tag{2.6}$$

B. Q-dependent warm Higgs inflation

In this subsection, we analyze the impact of the dissipation coefficient on the WHI. We start with the action of the Standard Model Higgs doublet H with a nonminimal coupling to gravity in the Jordan frame,

$$S_J = \int d^4x\sqrt{-g_J}\left[\frac{M_p^2}{2}\left(1 + 2\xi\frac{H^\dagger H}{M_p^2}\right)R_J + g_J^{\mu\nu}(D_\mu H)^\dagger(D_\nu H) - V(H)\right], \tag{2.7}$$

where M_p is the Planck mass, ξ is a coupling constant, R_J is the Ricci scalar, D_μ is the covariant derivative containing couplings with the gauge bosons, and $V(H)$ is the potential of the Higgs field, neglecting the mass term, i.e., $V(H) = \lambda|H|^4$. This choice is motivated by the understanding that the impact of the quadratic term relative to the quartic term on inflation is negligible during the inflationary process.

In the unitary gauge, employing the conformal transformation facilitates the conversion of the potential $V(H)$ to the Einstein frame [67–69], as below,

$$U \simeq \frac{\lambda M_p^4}{4\xi^2}\left(1 + \exp\left(-\sqrt{\frac{2}{3}}\frac{h}{M_p}\right)\right)^{-2}, \tag{2.8}$$

where λ is the self-coupling of the Higgs doublet.

In a thorough investigation of the slow-roll inflation process, through a analysis of the inflation potential, we get the slow-roll parameters (ε and η) and (ε_H and η_H), respectively corresponding to cold inflation and warm inflation,

$$\varepsilon = \frac{M_p^2}{2}\left(\frac{U'}{U}\right)^2, \qquad \eta = M_p^2\frac{U''}{U}; \tag{2.9}$$

$$\varepsilon_H = \frac{\varepsilon}{1+Q}, \qquad \eta_H = \frac{\eta}{1+Q}. \tag{2.10}$$

Furthermore, we can delineate the characteristics of the Universe during inflation, i.e. ($\varepsilon \ll 1$ and $\eta \ll 1$) as well as ($\varepsilon_H \ll 1$ and $\eta_H \ll 1$), which also ensures the flatness of the inflation potential. Once these conditions are violated, i.e. ($\varepsilon \approx 1$ or $\eta \approx 1$) as well as ($\varepsilon_H \approx 1$ or $\eta_H \approx 1$), the slow-roll process comes to an end, providing a framework for determining the field values at the conclusion of inflation.

In contrast to the cold scenario, the dissipative effects resulting from warm expansion will impact the scalar power spectrum. Detailed derivations can be found in the Refs. [46,70–73], and the final expression is as follows:

$$P_{\mathcal{R}}(k) = \left(\frac{H_k^2}{2\pi\dot{h}_k}\right)^2\mathcal{F}, \tag{2.11}$$

where $\mathcal{F}$ is the modified factor, and its specific form is given by

$$\mathcal{F} = \left(1 + 2n_k + \left(\frac{T_k}{H_k}\right)\frac{2\sqrt{3}\pi Q_k}{\sqrt{3+4\pi Q_k}}\right)G(Q_k), \tag{2.12}$$

where the subscript "k" denotes the time when the cosmological perturbation mode with wave number "k" exits the horizon during inflation. For the convenience of numerical computations in the next section, we establish a connection between each component in the scalar power spectrum and the Higgs inflaton field h, as detailed in the Appendix.

This dissipative effect has a negligible influence on the tensor power spectrum, which originates from the primordial tensor fluctuations of the metric. Its form aligns with the cold inflation model presented in Refs. [74,75] as

$$P_T(k) = \frac{16}{\pi}\left(\frac{H_k}{M_p}\right)^2. \tag{2.13}$$

Given the significant impact of dissipative effects on the scalar power spectrum during WHI, with negligible effects on the tensor power spectrum [58], it can be inferred that in this context, the tensor-to-scalar ratio (r) obtained through the ratio of tensor power spectrum to scalar power spectrum, and the spectral index (n_s) derived from the scalar power spectrum, will be modified. Specifically, these corrections can be summarized as follows [4]:

$$r = \left.\frac{P_T(k)}{P_{\mathcal{R}}(k)}\right|_{k=k_p} = \frac{16\epsilon}{(1+Q)^2}\mathcal{F}^{-1}. \tag{2.14}$$

$$n_s - 1 = \left.\frac{d\ln P_{\mathcal{R}}(k)}{d\ln k}\right|_{k=k_p} = \frac{1}{HP_{\mathcal{R}}}\frac{dP_{\mathcal{R}}}{dh}\dot{h}, \tag{2.15}$$

where k_p corresponds to the pivot scale.

C. Q dependent of relic gravitational waves

This section explores the influence of the dissipation coefficient on the relic gravitational waves (GWs). In general, the GWs energy density spectrum is written as

$$\Omega_{\rm GW}(\eta,k) = \frac{\rho_{\rm GW}(\eta,k)}{\rho_{\rm tot}(\eta)} = \frac{1}{24}\left(\frac{1}{a(\eta)H(\eta)}\right)^2\overline{P_h(\eta,k)}, \tag{2.16}$$

where $\overline{P_h(\eta,k)}$ is the power spectrum. For the WHI scenario, the expression for the GWs energy spectrum during the radiation-dominated era can be formulated through the utilization of the curvature perturbation power spectrum $P_{\mathcal{R}}(k)$ [Eq. (2.11)] dependent on Q as follows [76,77]:

$$\Omega_{\rm GW}(\eta,k) = \frac{1}{6}\int_0^\infty dv\int_{|1-v|}^{|1+v|}du\left(\frac{4v^2-(1+v^2-u^2)^2}{4uv}\right)^2 \times I^2(u,v)P_{\mathcal{R}}(ku)P_{\mathcal{R}}(kv). \tag{2.17}$$

Here,

$$I^2(u,v) = \frac{1}{2}\left(\frac{3(u^2+v^2-3)}{4u^3v^3}\right)^2 \times\left\{\left[-4uv+(u^2+v^2-3)\ln\left|\frac{3-(u+v)^2}{3-(u-v)^2}\right|\right]^2 + \pi^2(u^2+v^2-3)^2\Theta(v+u-\sqrt{3})\right\}, \tag{2.18}$$

where Θ is the Heaviside theta function.

Taking the thermal history of the Universe into consideration, one can get the GWs spectrum at present [76,78],

$$\Omega_{\rm GW,0}(k) = 0.39\times\Omega_{\gamma,0}\left(\frac{g_{\star,0}}{g_{\star,\rm eq}}\right)^{1/3}\Omega_{\rm GW}(\eta_{\rm eq},k), \tag{2.19}$$

where $\Omega_{\gamma,0}$ is the density parameter of radiation today, $g_{\star,0} = 3.36$ and $g_{\star,\rm eq} = 3.91$ are the effective numbers of relativistic degrees of freedom at the present time and at the time $\eta_{\rm eq}$ of the radiation-matter equality, respectively.

In order to facilitate a comparative analysis with gravitational waves experiments, we transform the variation of gravitational waves with respect to wave number k into a corresponding variation with respect to frequency f. The relationship between k and f is delineated as follows [78]:

$$f = \frac{k}{2\pi} = 1.5\times10^{-15}\left(\frac{k}{1\ \rm Mpc^{-1}}\right)\ \rm Hz. \tag{2.20}$$

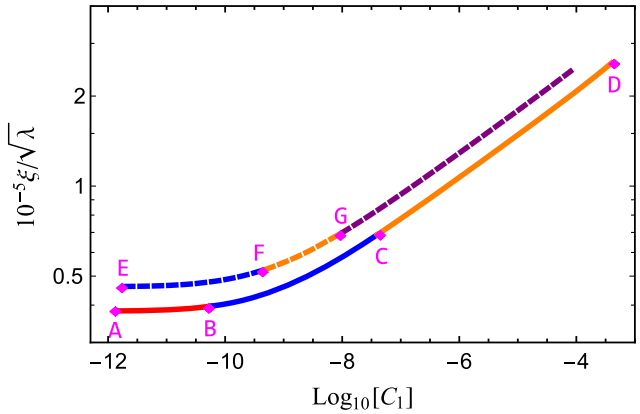

FIG. 1. The evolution of $\xi/\sqrt{\lambda}$ with respect to C_1 within the framework of the WHI model. The dashed line corresponds to $N_e = 60$, while the solid line corresponds to $N_e = 50$.

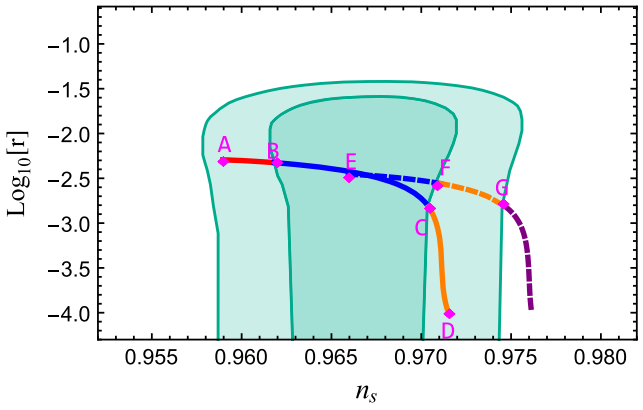

FIG. 2. The projections of warm inflation in the (n_s, r) planes are illustrated for both $N_e = 50$ and $N_e = 60$. The shaded regions represent the 1σ and 2σ experimental uncertainties from BAO, BICEP/KECK, and Planck data, with darker and lighter green denoting the respective confidence levels [80].

III. NUMERICAL DISCUSSION

In this section, we begin by constraining the model parameters of WHI using CMB, and then further investigate physical quantities such as r, n_s, and T, along with their dependence on Q.

A. Spectral index and tensor-to-scalar ratio

Figure 1 illustrates the viable parameter space of the WHI model under consideration of the amplitude of scalar fluctuations constraints, i.e., $P_{\mathcal{R}}|_{k=k_p} = 2.2 \times 10^{-9}$ [79]. The dashed line corresponds to $N_e = 60$, whereas the solid line corresponds to $N_e = 50$. To enrich the foundation of our forthcoming discussions, the precise values of C_1, $\xi/\sqrt{\lambda}$, and Q from point A to point G, kindly refer to Table I. Notably, the value of Q corresponds to the end of WHI. In the ensuing discourse, we scrutinize predictions associated with each of these points individually.

Upon substituting the model parameters depicted in Fig. 1 into Eqs. (2.14) and (2.15), we derive predictions for the model concerning (n_s, r). Predictions associated with the orange, blue, and purple model parameters in Fig. 1 correspond to the respective colors in Fig. 2, where solid lines represent $N_e = 50$ (dashed lines correspond to $N_e = 60$).

Notably, the predictions associated with the orange and blue fall within the 1σ and 2σ confidence intervals, respectively, while the purple predictions extend beyond the defined experimental regions. And the points A to G delineate the corresponding critical points.

Examination of Fig. 2 reveals that, with the constraint on the amplitude of scalar fluctuations, i.e., $P_{\mathcal{R}}|_{k=k_p} = 2.2 \times 10^{-9}$, the predictions for (n_s, r) under $N_e = 50$ align with experimental constraints. Conversely, for $N_e = 60$, certain predictions for (n_s, r) extend beyond the experimental limits, indicating a further refinement in constraining the model parameters.

B. Evolution of the different quantities

In Fig. 3, we employ the model parameter values from Table I to calculate the evolution of various quantities with respect to N, representing the dynamics of these quantities during the inflationary process. It is noteworthy that the evolution trends of these quantities are similar in the plots corresponding to points A, B, C, and D ($N_e = 50$) and points E, F, and G ($N_e = 60$), with the only distinction being in their specific numerical values.

Throughout the entire inflationary process, an observation of the four plots for points A, B, C, and D reveals that, as the model parameters $(C_1, \xi/\sqrt{\lambda})$ increase, the numerical value of Q also rises correspondingly. However, overall, Q remains at a relatively small level, i.e., $Q \ll 1$. This pattern is similarly evident for points E, F, and G. Consequently, WHI can be regarded as weak dissipation WHI.

TABLE I. The $(10^{10}C_1, 10^{-4}\xi/\sqrt{\lambda})$ value of the critical points (A, B, C, D, E, F, G) in Fig. 1.

Points	A	B	C	D	E	F	G
$10^{10}C_1$	0.0135	0.535	452	4.5×10^6	0.0175	4.45	94.5
$10^{-5}\xi/\sqrt{\lambda}$	0.38	0.39	0.69	2.58	0.46	0.52	0.69
$10^7 Q$	0.085	1.542	423.889	1.185×10^6	0.106	9.390	121.054

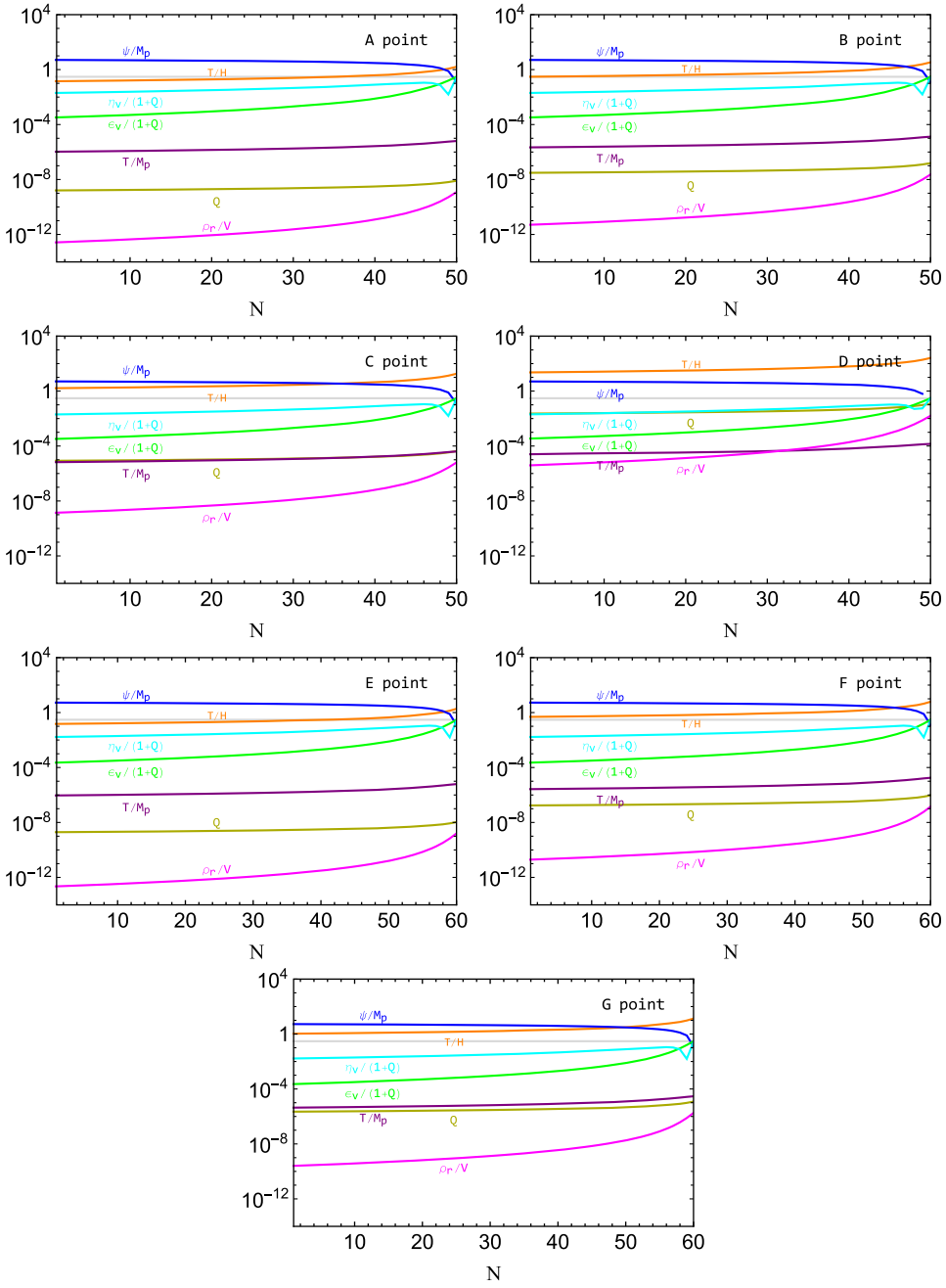

FIG. 3. The evolution of various parameters in the WHI scenario for A, B, C, D, E, F, and G points in the Fig. 1.

As WHI falls under the category of weak dissipation WHI, discussions should refrain from employing the strong dissipation approximation. Figure 3 illustrates that although the magnitude of Q is relatively small, the variation in its value under different parameters $\xi/\sqrt{\lambda}$, and C_1 is quite significant. Therefore, the parameters $(\rho_r/V, T/H, T/M_p)$ need to be studied carefully. More specifically, for the evolution of the temperature T/M_p during the inflationary period, the predictions for all points (A, B, C, D, E, F) nearly overlap, indicating that the model parameters $\xi/\sqrt{\lambda}$ and C_1 have a negligible influence on T/M_p. Under weak dissipation WHI, using Eq. (A5) for T, it can be inferred that Q has a minimal impact on T/M_p. Similarly, for the evolution of T/H, a comparable conclusion can be drawn from Eq. (A6). However, for the evolution of ρ_r/V, there are noticeable differences under different parameters $\xi/\sqrt{\lambda}$ and C_1, indicating that even with weak dissipative effects, the change in the radiation energy density relative to the potential energy is remarkably drastic. Therefore, in the study of WHI, the impact of Q should not be disregarded, even though it is relatively small.

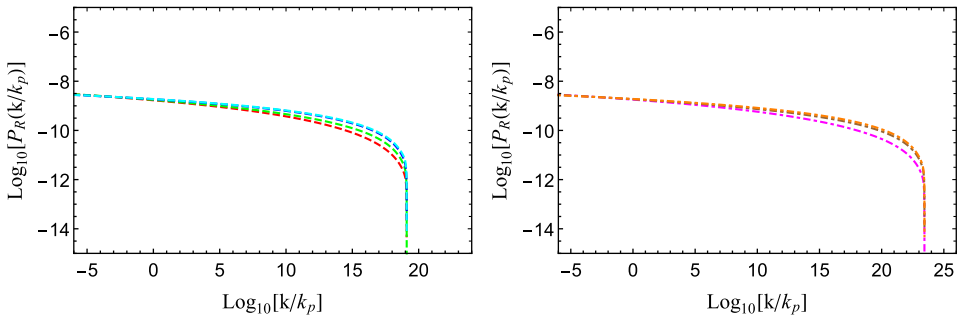

FIG. 4. The primordial curvature power spectrum, $P_R(k/k_p)$ vs $\ln(k/k_p)$ is presented in the left panel for $N_e = 50$ and in the right panel for $N_e = 60$.

C. Primordial curvature power spectrum

Utilizing the model parameter values from Table I and employing Eq. (2.11), we conduct an investigation of the primordial curvature power spectrum. We establish a connection between wave number k and inflationary field h by employing the relationship between N_k and k as given in Eq. (3.1), as well as the relationship between N_k and the inflationary field h,

$$N_k = \ln\frac{a_e}{a_k} = \ln\frac{a_e}{a_p} + \ln\frac{a_p}{a_k} = N_p + \ln\left(\frac{k_p}{k}\frac{H_k}{H_p}\right) = N_p - \ln\frac{k}{k_p} + \ln\frac{H_k}{H_p}. \quad (3.1)$$

The variation of $P_R(k/k_p)$ with $\ln(k/k_p)$ is illustrated in Fig. 4, where the dashed lines in red, green, blue, cyan, magenta, brown, and orange, respectively, correspond to the predictions associated with points A, B, C, D, E, F, and G.

It is noteworthy that the four dashed lines representing the $N_e = 50$ scenarios almost completely overlap, as do the corresponding lines for $N_e = 60$. This observation suggests that the model parameters $(C_1, \xi/\sqrt{\lambda})$ have a relatively minor impact on $P_R(k)$. Given that $(C_1, \xi/\sqrt{\lambda})$ can be translated into Q, this also implies that Q exerts a relatively small influence on $P_R(k)$. In the range of $\log_{10}(k/k_p) > 10$, there is a certain difference in the predicted primordial curvature power spectrum of several groups of parameters, but it is not significant, and the value of the primordial curvature power spectrum is very small, so it is a huge challenge for observation.

D. Relic gravitational wave spectrum

Figure 5 displays the spectrum of secondary gravitational waves at the present time. The dashed lines represent our predicted results, and for the four scenarios with $N_e = 50$, the differences in predicted gravitational waves are relatively small. Similarly, the three scenarios with $N_e = 60$ exhibit comparable trends. Additionally, the variation of r has a significant effect on the $\Omega_{\mathrm{GW},0}h^2$ of CI [81], while it has a small effect on WHI. The specific value of r for WHI can refer to Fig. 2. The main reason is that the difference of the primordial curvature power spectrum under different parameters is very small, ultimately resulting in a limited influence of Q on GWs. Despite the relatively modest amplitudes predicted by the model, there is potential for validation through future experiments, such as the SKA100, especially around the frequency $f \approx 10^{-9.5}$ Hz.

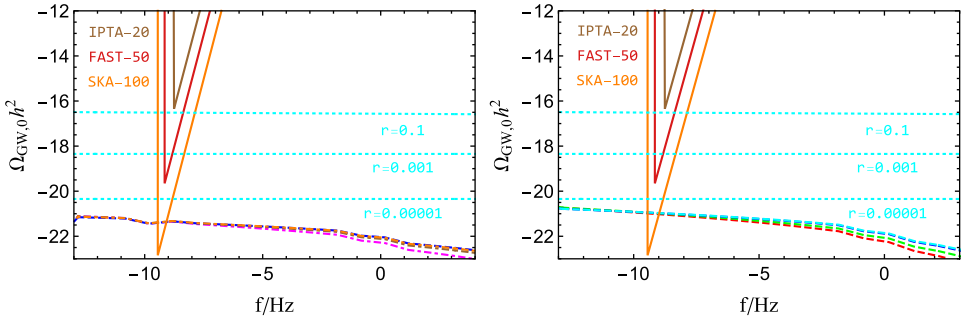

FIG. 5. The spectrum of secondary gravitational waves at the present time, as a function of frequency, are depicted with dashed lines indicating our predictive results. These predictions are calculated using Eq. (2.19) and are differentiated by the values of $N_e = 50$ and $N_e = 60$ for the left and right planes, respectively. The cyan dotted line is that of the CI predictions with different tensor-to-scalar ratio (r) [81]. The predictions of TPTA-20, FAST-50, and SKA-100 can refer to Refs. [63,82,83].

IV. SUMMARY

In this study, we investigate the dependencies of various physical quantities on Q during the WHI process. Recognizing the pivotal role of Q in WHI, we initially derive a relationship between each physical quantity in WHI and Q, avoiding any *a priori* assumptions regarding strong or weak dissipation.

Subsequently, accounting for the amplitude of scalar fluctuations' constraint, we determine the feasible parameter space $(C_1, \xi/\sqrt{\lambda})$. Further predictions of r and n_s are made and compared with the observations from CMB. We found that, for the scenario $N_e = 50$, the predictions completely conform to the constraints imposed by the CMB, while for the scenario $N_e = 60$, the predictions partially align within the CMB constraints.

Upon further analyzing the variation of the dissipation coefficient with N, we observe that although Q exhibit significant changes with variations in model parameters $(C_1, \xi/\sqrt{\lambda})$, overall, Q remained at extremely low levels, i.e., $Q \ll 1$. This indicates that Higgs warm inflation can be categorized as weakly dissipative warm inflation. Despite the small numerical value of Q, its dependence on various physical quantities under the influence of parameters $(C_1, \xi/\sqrt{\lambda})$, especially in the $N_e = 60$ scenario, is pronounced and should not be overlooked. This is clearly illustrated in Fig. 3.

Finally, we conduct an investigation into curvature perturbations during WHI process and find that Q had a negligible impact on them, further confirming the model's prediction of GWs variations. In addition, r has a significant impact on the $\Omega_{\mathrm{GW},0}h^2$ for CI, whereas this effect is relatively minor for WHI. Those conclusion is also well-reflected in Fig. 5, which additionally suggest that GWs generated by WHI are expected to be validated in future observational experiments, particularly through the detection capabilities of the SKA100 experiment.

ACKNOWLEDGMENTS

W. C. was supported by Chongqing Natural Science Foundation project under Grant No. CSTB2022NSCQ-MSX0432, by Science and Technology Research Project of Chongqing Education Commission under Grants No. KJQN202200621 and No. KJQN202200605, and by Chongqing Human Resources and Social Security Administration Program under Grant No. D63012022005. X.-W. C. was supported by Natural Science Foundation of Chongqing Grant No. cstc2021jcyjmsxmX0678, and by Science and Technology Research Program of Chongqing Municipal Education Commission Grant No. KJQN202201527. This work was also supported in part by the Fundamental Research Funds for the Central Universities under Grant No. 2021CDJQY-011, and by the National Natural Science Foundation of China under Grant No. 12147102. R. Z. was supported by supported by the National Natural Science Foundation of China under Grant No. 12305109, Chongqing Natural Science Foundation project under Grant No. CSTB2022NSCQ-MSX0534, and by Science and Technology Research Project of Chongqing Municipal Education Commission under Grant No. KJQN202300614.

APPENDIX

For the WHI, the more detailed information for each component in the scalar power spectrum is provided below.

For the investigation of the front factor $(\frac{H^2}{2\pi\dot{h}})$, the potential energy [Eq. (2.8)] serves to derive H, given by

$$H^2 = \frac{\lambda M_p^2}{12\xi^2\left(e^{-\frac{\sqrt{2}h}{M_p}}+1\right)^2}. \tag{A1}$$

Simultaneously, $\dot{h}$ can be calculated using Eq. (2.5), expressed as

$$\dot{h} \approx -\frac{U'(h)}{3(Q+1)H} = -\frac{\sqrt{2}M_p e^{\frac{\sqrt{2}h}{M_p}}\sqrt{\frac{\lambda M_p^2}{\xi^2}}}{3(Q+1)\left(e^{\frac{\sqrt{2}h}{M_p}}+1\right)^2}. \tag{A2}$$

Combining Eqs. (A1) and (A2), the front factor can ultimately be represented as follows:

$$\frac{H^2}{2\pi\dot{h}} = -\frac{(Q+1)e^{\frac{\sqrt{2}h}{M_p}}\sqrt{\frac{\lambda M_p^2}{\xi^2}}}{8\sqrt{2}\pi M_p}. \tag{A3}$$

Concerning the modified factor $(\mathcal{F})$ in Eq. (2.11),

$$\mathcal{F} = \left(1 + 2n_k + \left(\frac{T_k}{H_k}\right)\frac{2\sqrt{3}\pi Q_k}{\sqrt{3+4\pi Q_k}}\right)G(Q_k), \tag{A4}$$

where n represents the Bose-Einstein distribution function with a specific expression $n_k = 1/(\exp H_k/T_k - 1)$, and T denotes the temperature of the thermal bath. The temperature is intricately linked to the dissipative coefficient Q and the Hubble constant H. By solving the equation for the dissipative coefficient, $Q = \Gamma/3H = C_1 T/3H$, we can derive

$$T = \frac{1}{6^{1/4}}\left(\frac{\lambda Q M_p^4 e^{\frac{2\sqrt{2}h}{M_p}}}{C_r\xi^2(Q+1)^2(e^{\frac{\sqrt{2}h}{M_p}}+1)^4}\right)^{1/4}. \tag{A5}$$

Dividing the above relation with H, we obtain

$$\frac{T}{H} = 2^{3/4}3^{1/4}\left(\frac{\lambda M_p^2}{\xi^2\left(e^{-\frac{\sqrt{\frac{2}{3}}h}{M_p}}+1\right)^2}\right)^{-1/2} \times \left(\frac{\lambda Q M_p^4 e^{\frac{2\sqrt{\frac{2}{3}}h}{M_p}}}{\mathrm{Cr}\xi^2(Q+1)^2\left(e^{\frac{\sqrt{\frac{2}{3}}h}{M_p}}+1\right)^4}\right)^{1/4}. \quad \text{(A6)}$$

In a thermal bath, the interaction between the inflaton and radiation is characterized by the growth factor $G(Q_k)$. This function is introduced by Graham *et al.* [70], with subsequent discussions in studies [23,65]. The evolution of $G(Q_k)$ depends on Γ. In this work, we consider $\Gamma \propto T$, yielding the expression for $G(Q_k)$ in [23,26]

$$G(Q_k)_{\mathrm{linear}} = 1 + 0.0185Q_k^{2.315} + 0.335Q_k^{1.364}. \quad \text{(A7)}$$

In this study, we have observed the phenomenon of $Q \ll 1$ during the WHI epoch. Clearly, for small values of Q, i.e., $Q \ll 1$, it is noteworthy that the modified scalar power spectrum exhibits no significant variation with changes in Q.

Through a analysis of the aforementioned factors, it is evident that all these factors can be expressed in terms of model parameters the nonminimal coupling ξ, the coupling λ, the field h, and the dissipation coefficient Q. Subsequently, based on the definition of the dissipation coefficient $Q = \Gamma/3H = C_1T/3H$ and in conjunction with the Eq. (A5), the dissipation coefficient Q is formulated in terms of ξ, λ, and h,

$$e^{\frac{\sqrt{\frac{2}{3}}h}{M_p}} \approx \frac{2\sqrt{\frac{2}{3}}C_1^2\xi}{3\sqrt{\frac{g_\star\pi^2}{30}}\sqrt{\lambda}Q^{5/2}} \rightarrow Q = \frac{\left(\frac{2}{3}\right)^{3/5}C_1^{4/5}\xi^{2/5}}{\left(\frac{g_\star\pi^2}{30}\right)^{1/5}\lambda^{1/5}}e^{-\frac{2\sqrt{\frac{2}{3}}h}{5M_p}}. \quad \text{(A8)}$$

Therefore, the scalar power spectrum is entirely characterized by the model parameters ξ, λ, and the field h.

[1] A. H. Guth, The inflationary universe: A possible solution to the horizon and flatness problems, Phys. Rev. D **23**, 347 (1981).
[2] A. D. Linde, A new inflationary universe scenario: A possible solution of the horizon, flatness, homogeneity, isotropy and primordial monopole problems, Phys. Lett. **108B**, 389 (1982).
[3] A. D. Linde, Chaotic inflation, Phys. Lett. **129B**, 177 (1983).
[4] M. AlHallak, K. K. A. Said, N. Chamoun, and M. S. El-Daher, On warm natural inflation and Planck 2018 constraints, Universe **9**, 80 (2023).
[5] W. Cheng and L. Bian, From inflation to cosmological electroweak phase transition with a complex scalar singlet, Phys. Rev. D **98**, 023524 (2018).
[6] W. Cheng and L. Bian, Higgs inflation and cosmological electroweak phase transition with N scalars in the post-Higgs era, Phys. Rev. D **99**, 035038 (2019).
[7] W. Cheng, X. Liu, and R. Zhou, Non-minimal coupling inflation and dark matter under the $\mathbb{Z}_3$ symmetry, J. Cosmol. Astropart. Phys. 05 (2023) 049.
[8] W. Cheng, T. Qin, J. Jiang, and R. Zhou, Constraints on real scalar inflation from preheating of LATTICEEASY, arXiv:2212.12851.
[9] S. Khan, J. Kim, and P. Ko, Interplay between Higgs inflation and dark matter models with dark $U(1)$ gauge symmetry, arXiv:2309.07839.
[10] J. G. Rodrigues, V. Oliveira, R. von Marttens, C. A. d. S. Pires, and J. Alcaniz, CMB constraints on inflection-point inflation with a pseudo-scalar dark matter, arXiv:2309.09842.
[11] H. Zhou, Q. Yu, Y. Pan, R. Zhou, and W. Cheng, Reheating constraints on modified single-field natural inflation models, Eur. Phys. J. C **82**, 588 (2022).
[12] V. K. Oikonomou, $f(R)$-gravity generated post-inflationary eras and their effect on primordial gravitational waves, Ann. Phys. (Berlin) **534**, 2200134 (2022).
[13] K. Kannike, A. Kubarski, L. Marzola, and A. Racioppi, A minimal model of inflation and dark radiation, Phys. Lett. B **792**, 74 (2019).
[14] Y. Ema, Higgs scalaron mixed inflation, Phys. Lett. B **770**, 403 (2017).
[15] O. Lebedev and H. M. Lee, Higgs portal inflation, Eur. Phys. J. C **71**, 1821 (2011).
[16] X. Calmet and I. Kuntz, Higgs Starobinsky inflation, Eur. Phys. J. C **76**, 289 (2016).
[17] F. L. Bezrukov and M. Shaposhnikov, The standard model Higgs boson as the inflaton, Phys. Lett. B **659**, 703 (2008).
[18] X.-B. Li, H. Wang, and J.-Y. Zhu, Gravitational waves from warm inflation, Phys. Rev. D **97**, 063516 (2018).
[19] X.-B. Li, X.-G. Zheng, and J.-Y. Zhu, Spectra and entropy of multifield warm inflation, Phys. Rev. D **99**, 043528 (2019).
[20] A. N. Taylor and A. Berera, Perturbation spectra in the warm inflationary scenario, Phys. Rev. D **62**, 083517 (2000).
[21] A. Berera, Interpolating the stage of exponential expansion in the early universe: A possible alternative with no reheating, Phys. Rev. D **55**, 3346 (1997).

[22] A. Berera, Warm inflation at arbitrary adiabaticity: A model, an existence proof for inflationary dynamics in quantum field theory, Nucl. Phys. **B585**, 666 (2000).
[23] M. Bastero-Gil, A. Berera, R. Hernández-Jiménez, and J. G. Rosa, Dynamical and observational constraints on the warm little inflaton scenario, Phys. Rev. D **98**, 083502 (2018).
[24] M. Bastero-Gil and A. Berera, Warm inflation model building, Int. J. Mod. Phys. A **24**, 2207 (2009).
[25] M. Levy, J. G. Rosa, and L. B. Ventura, Warm inflation, neutrinos and dark matter: A minimal extension of the standard model, J. High Energy Phys. 12 (2021) 176.
[26] M. Benetti and R. O. Ramos, Warm inflation dissipative effects: Predictions and constraints from the Planck data, Phys. Rev. D **95**, 023517 (2017).
[27] V. F. Mukhanov and G. V. Chibisov, Quantum fluctuations and a nonsingular universe, JETP Lett. **33**, 532 (1981).
[28] A. A. Starobinsky, Dynamics of phase transition in the new inflationary universe scenario and generation of perturbations, Phys. Lett. **117B**, 175 (1982).
[29] A. H. Guth and S. Y. Pi, Fluctuations in the new inflationary universe, Phys. Rev. Lett. **49**, 1110 (1982).
[30] J. M. Bardeen, P. J. Steinhardt, and M. S. Turner, Spontaneous creation of almost scale—free density perturbations in an inflationary universe, Phys. Rev. D **28**, 679 (1983).
[31] L. F. Abbott and M. B. Wise, Constraints on generalized inflationary cosmologies, Nucl. Phys. **B244**, 541 (1984).
[32] L. F. Abbott and M. B. Wise, Large scale anisotropy of the microwave background and the amplitude of energy density fluctuations in the early universe, Astrophys. J. Lett. **282**, L47 (1984).
[33] A. Albrecht and P. J. Steinhardt, Cosmology for grand unified theories with radiatively induced symmetry breaking, Phys. Rev. Lett. **48**, 1220 (1982).
[34] K. Sato, Cosmological baryon number domain structure and the first order phase transition of a vacuum, Phys. Lett. **99B**, 66 (1981).
[35] B. A. Bassett, S. Tsujikawa, and D. Wands, Inflation dynamics and reheating, Rev. Mod. Phys. **78**, 537 (2006).
[36] R. Allahverdi, R. Brandenberger, F.-Y. Cyr-Racine, and A. Mazumdar, Reheating in inflationary cosmology: Theory and applications, Annu. Rev. Nucl. Part. Sci. **60**, 27 (2010).
[37] M. A. Amin, M. P. Hertzberg, D. I. Kaiser, and J. Karouby, Nonperturbative dynamics of reheating after inflation: A review, Int. J. Mod. Phys. D **24**, 1530003 (2014).
[38] M. Drewes and J. U. Kang, The kinematics of cosmic reheating, Nucl. Phys. **B875**, 315 (2013); **B888**, 284(E) (2014).
[39] M. Drewes, On finite density effects on cosmic reheating and moduli decay and implications for dark matter production, J. Cosmol. Astropart. Phys. 11 (2014) 020.
[40] A. R. Liddle and D. H. Lyth, *Cosmological Inflation and Large-Scale Structure* (Cambridge University Press, Cambridge, England, 2000).
[41] A. Berera, Thermal properties of an inflationary universe, Phys. Rev. D **54**, 2519 (1996).
[42] A. Berera, The warm inflationary universe, Contemp. Phys. **47**, 33 (2006).
[43] A. Berera, Developments in inflationary cosmology, Pramana **72**, 169 (2009).
[44] A. Berera, M. Gleiser, and R. O. Ramos, Strong dissipative behavior in quantum field theory, Phys. Rev. D **58**, 123508 (1998).
[45] L. M. H. Hall, I. G. Moss, and A. Berera, Constraining warm inflation with the cosmic microwave background, Phys. Lett. B **589**, 1 (2004).
[46] L. M. H. Hall, I. G. Moss, and A. Berera, Scalar perturbation spectra from warm inflation, Phys. Rev. D **69**, 083525 (2004).
[47] A. Berera, I. G. Moss, and R. O. Ramos, Warm inflation and its microphysical basis, Rep. Prog. Phys. **72**, 026901 (2009).
[48] M. Bastero-Gil, A. Berera, R. O. Ramos, and J. G. Rosa, General dissipation coefficient in low-temperature warm inflation, J. Cosmol. Astropart. Phys. 01 (2013) 016.
[49] S. Bartrum, A. Berera, and J. G. Rosa, Warming up for Planck, J. Cosmol. Astropart. Phys. 06 (2013) 025.
[50] I. Dymnikova and M. Khlopov, Self-consistent initial conditions in inflationary cosmology, Gravitation Cosmol. **4**, 50 (1998).
[51] I. Dymnikova and M. Khlopov, Decay of cosmological constant as Bose condensate evaporation, Mod. Phys. Lett. A **15**, 2305 (2000).
[52] I. Dymnikova and M. Khlopov, Decay of cosmological constant in self-consistent inflation, Eur. Phys. J. C **20**, 139 (2001).
[53] A. Berera, Warm inflation, Phys. Rev. Lett. **75**, 3218 (1995).
[54] A. Berera and L.-Z. Fang, Thermally induced density perturbations in the inflation era, Phys. Rev. Lett. **74**, 1912 (1995).
[55] W. Cheng, L. Bian, and Y.-F. Zhou, Axionlike particle inflation and dark matter, Phys. Rev. D **104**, 063010 (2021).
[56] W. Cheng, T. Qian, Q. Yu, H. Zhou, and R.-Y. Zhou, Gravitational wave from axionlike particle inflation, Phys. Rev. D **104**, 103502 (2021).
[57] G. Montefalcone, V. Aragam, L. Visinelli, and K. Freese, Constraints on the scalar-field potential in warm inflation, Phys. Rev. D **107**, 063543 (2023).
[58] V. Kamali, M. Motaharfar, and R. O. Ramos, Recent developments in warm inflation, Universe **9**, 124 (2023).
[59] O. Grøn, Warm inflation, Universe **2**, 20 (2016).
[60] V. Kamali, Non-minimal Higgs inflation in the context of warm scenario in the light of Planck data, Eur. Phys. J. C **78**, 975 (2018).
[61] D. Samart, P. Ma-adlerd, and P. Channuie, Warm Higgs–Starobinsky inflation, Eur. Phys. J. C **82**, 122 (2022).
[62] T. Eadkhong, P. Dam-O, P. Channuie, and D. Momeni, Nonminimally-coupled warm Higgs inflation: Metric vs. Palatini formulations, Nucl. Phys. **B994**, 116289 (2023).
[63] C. L. Carilli and S. Rawlings, Science with the square kilometer array: Motivation, key science projects, standards and assumptions, New Astron. Rev. **48**, 979 (2004).
[64] Y. Zhang, Warm inflation with a general form of the dissipative coefficient, J. Cosmol. Astropart. Phys. 03 (2009) 023.
[65] M. Bastero-Gil, A. Berera, and R. O. Ramos, Shear viscous effects on the primordial power spectrum from warm inflation, J. Cosmol. Astropart. Phys. 07 (2011) 030.
[66] A. Berera and R. O. Ramos, The affinity for scalar fields to dissipate, Phys. Rev. D **63**, 103509 (2001).

[67] E. Elizalde and S. D. Odintsov, Renormalization group improved effective Lagrangian for interacting theories in curved space-time, Phys. Lett. B **321**, 199 (1994).
[68] E. Elizalde, S. D. Odintsov, E. O. Pozdeeva, and S. Y. Vernov, Renormalization-group improved inflationary scalar electrodynamics and SU(5) scenarios confronted with Planck 2013 and BICEP2 results, Phys. Rev. D **90**, 084001 (2014).
[69] S. Choubey and A. Kumar, Inflation and dark matter in the inert doublet model, J. High Energy Phys. 11 (2017) 080.
[70] C. Graham and I. G. Moss, Density fluctuations from warm inflation, J. Cosmol. Astropart. Phys. 07 (2009) 013.
[71] R. O. Ramos and L. A. da Silva, Power spectrum for inflation models with quantum and thermal noises, J. Cosmol. Astropart. Phys. 03 (2013) 032.
[72] L. Visinelli, Observational constraints on monomial warm inflation, J. Cosmol. Astropart. Phys. 07 (2016) 054.
[73] I. G. Moss and C. Xiong, Non-Gaussianity in fluctuations from warm inflation, J. Cosmol. Astropart. Phys. 04 (2007) 007.
[74] W. H. Kinney, Cosmology, inflation, and the physics of nothing, NATO Sci. Ser. II **123**, 189 (2003).
[75] S. Dodelson, *Modern Cosmology* (Academic Press, Amsterdam, 2003).
[76] K. Kohri and T. Terada, Semianalytic calculation of gravitational wave spectrum nonlinearly induced from primordial curvature perturbations, Phys. Rev. D **97**, 123532 (2018).
[77] Z.-Z. Peng, C. Fu, J. Liu, Z.-K. Guo, and R.-G. Cai, Gravitational waves from resonant amplification of curvature perturbations during inflation, J. Cosmol. Astropart. Phys. 10 (2021) 050.
[78] M. Correa, M. R. Gangopadhyay, N. Jaman, and G. J. Mathews, Induced gravitational waves via warm natural inflation, arXiv:2306.09641.
[79] P. A. R. Ade *et al.* (Planck Collaboration), Planck 2015 results. XIII. Cosmological parameters, Astron. Astrophys. **594**, A13 (2016).
[80] P. A. R. Ade *et al.* (BICEP, Keck Collaborations), Improved constraints on primordial gravitational waves using Planck, WMAP, and BICEP/Keck observations through the 2018 observing season, Phys. Rev. Lett. **127**, 151301 (2021).
[81] X.-J. Liu, W. Zhao, Y. Zhang, and Z.-H. Zhu, Detecting relic gravitational waves by Pulsar Timing Arrays: Effects of cosmic phase transitions and relativistic free-streaming gases, Phys. Rev. D **93**, 024031 (2016).
[82] R. Nan, D. Li, C. Jin, Q. Wang, L. Zhu, W. Zhu, H. Zhang, Y. Yue, and L. Qian, The Five-Hundred-Meter Aperture Spherical Radio Telescope (FAST) project, Int. J. Mod. Phys. D **20**, 989 (2011).
[83] https://ipta4gw.org/?page_id=89.